LOW-TEMPERATURE
PLASMA

Hydrocarbon Plasma Chemistry
in a Continuous Microwave Discharge

**A. M. Gorbachev, A. B. Muchnikov, A. L. Vikharev,
D. B. Radishchev, and V. A. Koldanov**

Institute of Applied Physics, Russian Academy of Sciences, ul. Ul'yanova 46, Nizhni Novgorod, 603950 Russia
Received December 8, 2006

Abstract—A study is made of the relation between the kinetic processes involving carbon-containing species and the intensity ratios of different emission lines in synthesizing diamond films in a microwave discharge plasma. The intensity ratios of the emission lines are measured as functions of the pressure, composition, and flow rate of the gas mixture. The kinetic processes involving carbon-containing components are simulated under conditions close to the experimental ones. It is shown that the intensity ratios of different pairs of lines can be used to control diamond film deposition.

1. INTRODUCTION

Rapid development of the technology for chemical vapor deposition (CVD) of diamond films in microwave discharge plasmas stimulated studies on the plasmachemistry of carbon-containing radicals. The deposition of diamond films (DFs) in reactors is monitored by using optical absorption spectroscopy [1], optical emission spectroscopy [2], and laser induced fluorescence (LIF) [3]. The most simple and available among these methods is emission spectroscopy, which is widely used to control DF deposition [4–8]. However, detailed information on how the emission intensities of different components are related to the plasma chemical composition, deposition rate, and DF quality is still lacking. The aim of this study was to investigate the relation between the kinetic processes involving carbon-containing species and the intensity ratios of different emission lines in a microwave discharge plasma, as well as to examine the possibility of using these ratios to monitor DF deposition.

2. EXPERIMENTAL SETUP
AND DIAGNOSTIC TECHNIQUE

The experimental facility for studying DF deposition was described in detail in [9]. A hydrogen–methane gas mixture was supplied into a quartz tube placed in a cylindrical cavity. The cavity was excited at the TM_{013} mode by a magnetron operating at a frequency of 2.45 GHz. As a result, a continuous microwave discharge was ignited and sustained in the tube. The hemispherical discharge plasma contacted a silicon substrate, on which a DF was deposited. The temperature regime required for DF deposition was achieved by varying the thermal resistance between the substrate and cooling water. The substrate temperature was measured by an IR pyrometer.

Our experiments were performed at a microwave power of 3 kW and gas-mixture pressures of 60–130 Torr. The microphotograph and Raman spectrum of a typical diamond film deposited under these conditions are shown in Fig. 1.

The discharge plasma was investigated by using optical emission spectroscopy: the emission was output through the cavity window, was focused by a lens into an optical fiber, and was then fed to the entrance slit of a SOLAR TII MS 3504 monochromator. At the exit slit of the monochromator, a broadband Hamamatsu R298 PMT or an LD 3648 detector based on a TCD 1304AP (Toshiba) CCD array was installed.

Figure 2 shows a typical optical emission spectrum from a continuous microwave discharge in hydrogen with a small additive of methane. The parameters of the emission lines of different plasma components are listed in the table.

When the gas density is so high that collisional quenching of the upper levels prevails over their radiative decay and the excitation proceeds from the ground state, the emission intensity of the ith component of the plasma of a continuous discharge can be expressed as follows:

$$I_i \propto \xi N_i^*, \quad N_i^* = \frac{k_i^{ex} N_i N_i^{ex}}{k_i^{qu} N}, \qquad (1)$$

where N_i^* is the density of excited particles; N_i is the density of the particles in the ground state; k_i^{ex} and k_i^{qu} are the excitation and quenching rate constants, respec-

(a)

10 μm

(b)
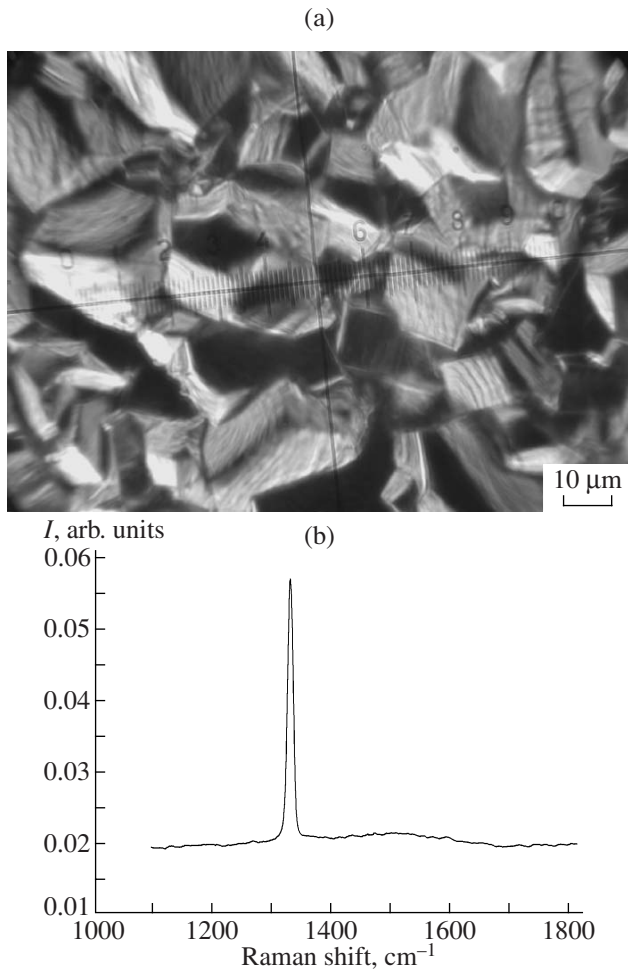
Fig. 1. (a) Typical microphotograph and (b) Raman spectrum of a diamond film.

tively; N_i^{ex} is the density of the particles that collisionally excite the ith component; N is the density of the molecules that quench the excited level; and ξ is a form factor that takes into account the plasma volume from which emission is recorded. To exclude the form factor ξ, it is reasonable to use the intensity ratios rather than the absolute intensities themselves,

$$\frac{I_i}{I_j} \propto \frac{N_i^*}{N_j^*} \propto \frac{N_i}{N_j}\left[\frac{k_i^{\mathrm{ex}}k_j^{\mathrm{qu}}N_i^{\mathrm{ex}}}{k_i^{\mathrm{qu}}k_j^{\mathrm{ex}}N_j^{\mathrm{ex}}}\right]. \qquad (2)$$

Under our experimental conditions (i.e., at pressures of a few tens of Torr), the emitting levels are mainly quenched in collisions with molecules. In this case, variations in the discharge parameters only slightly affect the ratio between the quenching rate constants.

The emitting levels are excited (i) by electron impact from the ground state, (ii) in collisions with molecules, and (iii) via chemiluminescence [10, 11].

Variations in the plasma parameters ratio only slightly affect the rate constants for electron-impact excitation into levels with close excitation thresholds; in this case, the intensity ratio is proportional to the ratio of the relevant concentrations. This property is employed in the well-known actinometry technique for measuring the concentrations of various discharge components [12] (e.g., of hydrogen atoms [9]). The ratio between the rate constants for electron-impact excitation into levels with significantly different excitation thresholds is also slightly affected by the plasma parameters, provided that the electron distribution function (EDF) remains unchanged.

When the levels are excited in collisions with molecules, a decisive factor is the gas-mixture temperature. Numerical simulations [13] show that the gas temperature is limited from above at a level of 2500–2700 K due to thermal dissociation of hydrogen in the reaction

$$H_2 + N \longleftrightarrow H + H + N, \qquad (3)$$
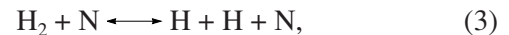
which consumes an energy of 4.8 eV when going in the forward direction. In this case, the excitation rate of the emitting levels is again only slightly affected by the discharge parameters.

In our experiments, we varied the methane percentage in the mixture, the gas flow rate, and the gas pres-

Plasma components of a microwave discharge in an $H_2 + CH_4$ mixture and the corresponding wavelengths of the plasma emission lines

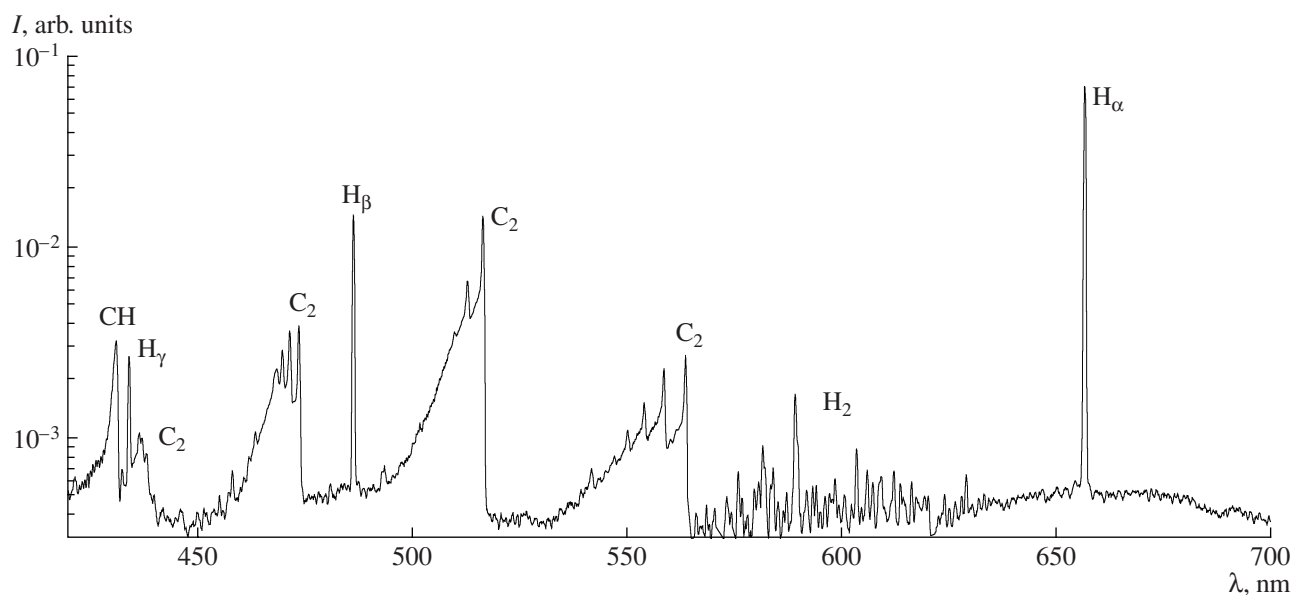| Name		Wavelength, nm	Excitation threshold, eV
Atomic hydrogen	H_α	656.3	12.098
(Balmer-series lines)	H_β	486.1	12.760
	H_γ	434.0	13.065
CH radical ($A^2\Delta$–$X^2\Pi$)	$\Delta v = 0$	~431	2.87
C$_2$ radical ($d^3\Pi_g$–$a^3\Pi_u$)	$\Delta v = 0$	~516	2.48
	$\Delta v = 1$	~475	2.48
	$\Delta v = -1$	~564	2.48
	$\Delta v = 2$	~437	2.48
Argon Ar($2p_9$–$1s_5$)		811.5	13.08

Fig. 2. Typical emission spectrum from the plasma of a microwave discharge in hydrogen with a small additive of methane.

sure in the reactor. Variations in the first two parameters practically do not affect both the EDF and the gas temperature; as a result, intensity ratios (2) are proportional to the ratios between the corresponding concentrations.

As the pressure increases, whereas the gas temperature varies slightly, the density of molecules increases in proportion to the pressure. Calculations [13] and measurements [14] also show that the electron density increases in proportion to the pressure. Hence, the rates of both electron-impact excitation and excitation in collisions with molecules are proportional to the pressure, so the intensity ratio is equal to the concentration ratio.

That the emission intensity is proportional to the concentration is confirmed experimentally. The concentration of carbon-containing species was measured by using absorption spectroscopy [15, 16], mass-spectroscopy [17], and cavity ring-down spectroscopy [18]. In those studies, the plasma parameters (such as the gas-mixture composition, pressure, and substrate temperature) were varied and the intensity of the (0,0) rotational band of the Swan system of C_2 radicals (with a wavelength of about 516 nm) was compared with the measured concentration of C_2 radicals or acetylene (C_2H_2) molecules. In [15–18], it was claimed that, within a wide range of experimental conditions, the emission intensity of C_2 radicals is proportional (or nearly proportional) to the concentration of C_2 radicals in the ground state or the concentration of C_2H_2 molecules. Note that, in [15–18], the experiments were performed under very different conditions; nevertheless, in some experiments, the experimental conditions were close to the conditions of our experiments. Therefore, we will assume that the intensity ratios are nearly pro-

portional to the concentration ratios of the relevant mixture components.

3. EXPERIMENTAL RESULTS

In our experiments, we measured the intensity ratios between the atomic hydrogen lines and the edges of the emission bands of carbon-containing radicals CH and C_2 as functions of the pressure and composition of the gas mixture (Fig. 3), as well as of the gas flow rate in the reactor (Fig. 4).[1] Note that, in all the experiments, the intensity ratios of the H_α, H_β, and H_γ lines always remained unchanged. This indicates that variations in the discharge parameters slightly affects the EDF.

Taking into account the important role of atomic hydrogen in DF synthesis [19], we measured the degree of hydrogen dissociation [H]/[H_2] under different deposition conditions by using the actinometry method [9]. A small additive of argon (up to 10%) was used as an actinometer. The degree of dissociation of H_2 was assumed to be proportional to the intensity ratio of the H_γ and Ar 8115-Å lines, which have nearly the same excitation thresholds (see table and [9, 20]).

It can be seen from Fig. 3a that the ratio I_{H_γ}/I_{Ar} somewhat increases as the methane percentage increases to 0.5%, after which the intensity ratio remains unchanged. The increase in the degree of dissociation with increasing methane concentration is related to the change of the main ion species in the plasma; this results an increase in the recombination rate constant and a change in the diffusion coefficient.

---

[1] Figures 3 and 4 also present results of numerical simulations that will be discussed in the next section.
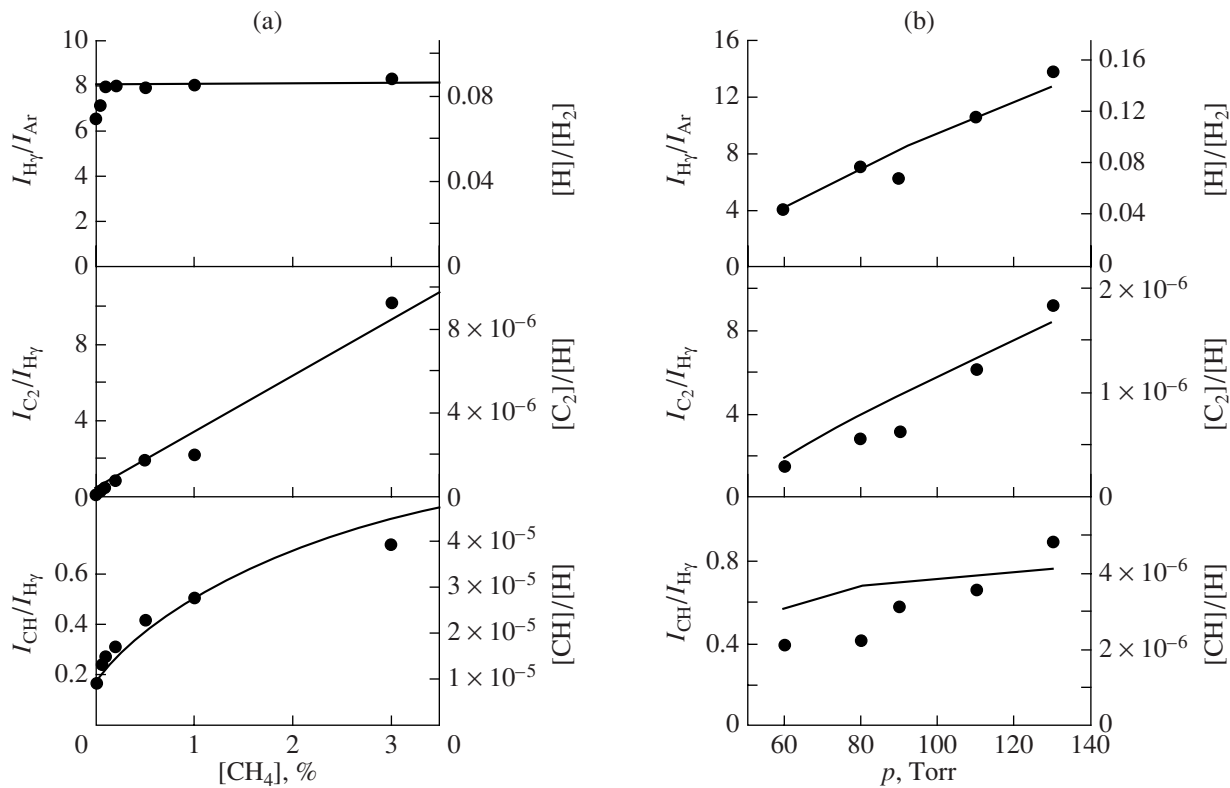
Fig. 3. Measured intensity ratios $I_{H\gamma}/I_{Ar}$, $I_{C_2}/I_{H\gamma}$, and $I_{CH}/I_{H\gamma}$ (symbols) and the corresponding calculated concentration ratios (solid curves) as functions of (a) the methane percentage in the mixture at a pressure of $p = 90$ Torr and (b) the pressure of the 1%[CH$_4$]/[H$_2$] mixture at a hydrogen flow rate of 200 sccm.
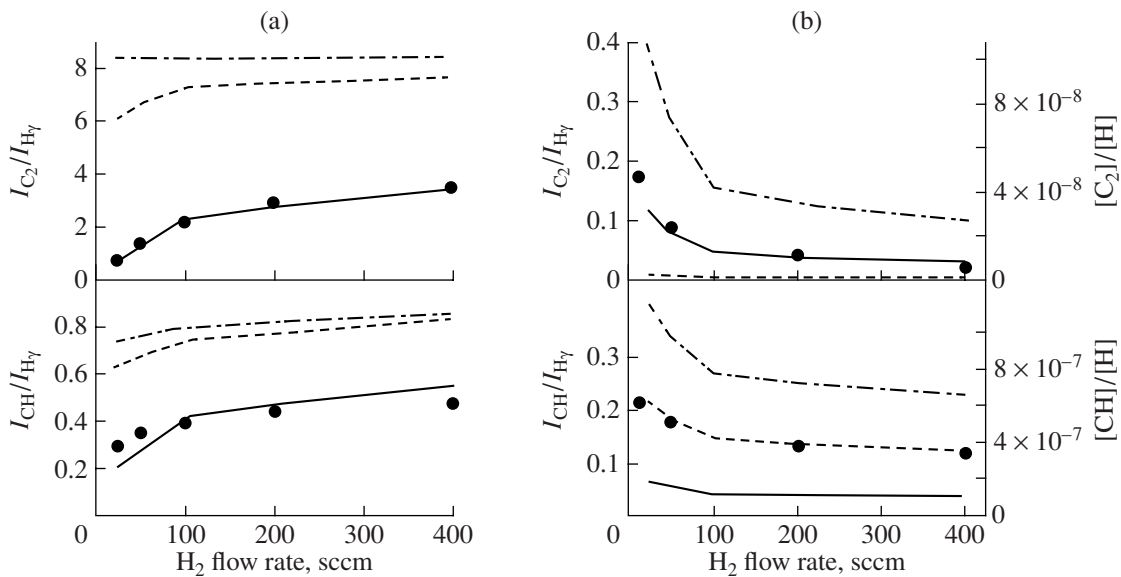
Fig. 4. Line intensity ratios and the corresponding calculated concentration ratios as functions of the gas flow rate in the reactor: (a) hydrogen with a 1% methane additive (the circles show the experimental data, and the solid, dashed, and dashed-and-dotted curves correspond to the simulation results obtained at $\tau_{CH_3} = 0.01$ s, 0.1 s, and ∞, respectively; (b) pure hydrogen (the circles show the experimental data, and the solid, dashed, and dashed-and-dotted curves correspond to the simulation results obtained at $I_C = 1.7 \times 10^{12}$, 1.7×10^{11}, and 5.6×10^{12} sccm, respectively.
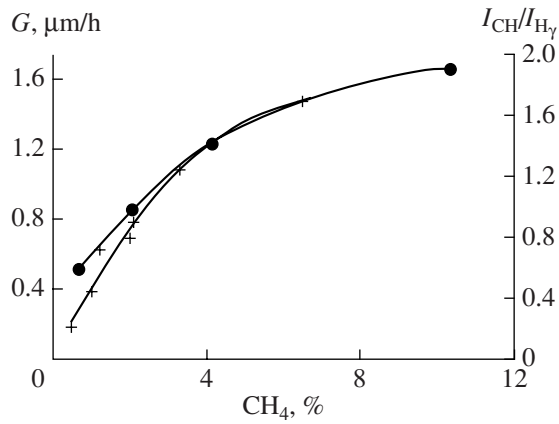
Fig. 5. DF growth rate (circles) and intensity ratio $I_{CH}/I_{H\gamma}$ (crosses) vs. methane percentage in the mixture.

The latter leads to a decrease in the plasma volume and an increase in the electron density [9, 11]. It can be seen from Fig. 3b that the degree of dissociation of H_2 is a linear function of the gas pressure. This is because an increase in the pressure leads to a decrease in the plasma volume and an increase in the microwave power density (or specific power) and electron density; accordingly, the rate of electron-impact dissociation of H_2 increases [9, 13].

The intensities ratios I_{CH}/I_{H_γ} and I_{C_2}/I_{H_γ} increase with both the methane percentage and the gas pressure. The ratio I_{C_2}/I_{H_γ} increases faster than I_{CH}/I_{H_γ}, being proportional to the methane percentage.

It can be seen from Fig. 3a that the emission intensity of CH radicals is nonzero at a zero methane percentage. Seemingly, this is caused by the influx of carbon into the gas phase from the reactor wall and DF surface. We will discuss this effect in more detail in Section 4.

Figure 5 shows the DF growth rate and the intensity ratio I_{CH}/I_{H_γ} as functions of the methane percentage. It can be seen that both quantities increase in a similar manner with increasing methane percentage in the mixture.

The dependences of the line intensities on the gas-mixture flow rate in the reactor were measured at a constant methane percentage (Fig. 4a) and in pure hydrogen (Fig. 4b). In the former case, the emission intensities of carbon-containing components increase with increasing gas flow rate. Presumably, this is related to the deposition of carbon on the DF surface, whereas the increase in the line intensities is caused by an increase in the supply rate of carbon into the reactor. In pure hydrogen, the decrease in the emission intensities of hydrocarbon components is related to the influx of carbon from the DF surface into the plasma volume and its subsequent pumping-out. The decrease in the carbon concentration can also be related to the cleaning of the surface from carbon; however, this process is too slow to play any role during our measurements.

4. NUMERICAL SIMULATIONS

The processes involving carbon-containing species were analyzed by using a zero-dimensional model of the chemical kinetics of neutral components. Charged species were ignored because, at pressures of a few tens of Torr, the densities of charged particles are several orders of magnitude lower than those of neutrals [19]. In simulations, we took into account the following gas-mixture components: H_2, H, CH_4, CH_3, CH_2, CH, C, C_2H_6, C_2H_5, C_2H_4, C_2H_3, C_2H_2, C_2H, and C_2. Components containing three and more carbon atoms were ignored because, under our experimental conditions, their concentrations were low [19]. A scheme of the reactions incorporated in the model is shown in Fig. 6. The reactions can be divided unto two groups: fast and slow ones. The characteristic time of fast reactions is $\tau_{fast} \cong 0.1$ ms, whereas that of slow reactions is $\tau_{slow} \sim 10$ ms, i.e., two orders of magnitude longer. The rate constants for forward reactions were taken from [21–24]. The rate constants for reverse reactions were calculated from the principle of detailed balance.

Atomic hydrogen plays an important role in DF synthesis [19], because it is involved in most of the reactions shown in Fig. 6. Under our experimental condi-
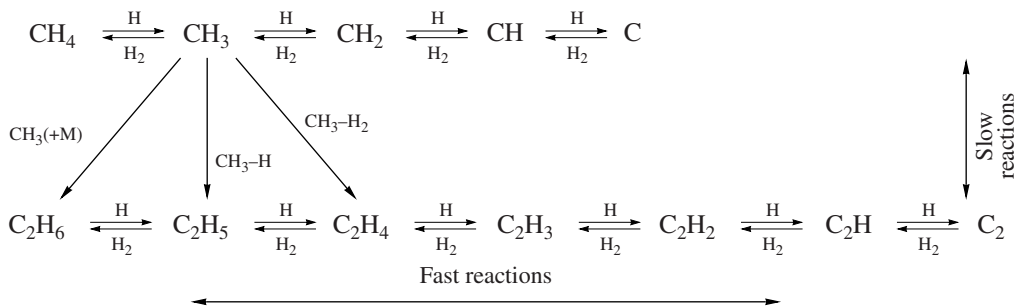

Fig. 6. Scheme of the conversion reactions of carbon-containing species incorporated in the model.

tions, atomic hydrogen is mainly produced via electron-impact and thermal dissociation of molecular hydrogen. In the model, the density of hydrogen atoms was found from the equation

$$\frac{\partial[H]}{\partial t} = k_d^*[H_2]N_e - 2k_R[H]^2N - \nu_d[H] + k_T[H_2]N. \tag{4}$$

Here, k_d^* is the rate constant for electron-impact dissociation (with allowance for the dissociation of both ground-state and vibrationally excited molecules), k_R is the rate constant for triple recombination, k_T is the rate constant for thermal dissociation, N is the density of gas molecules, and $\nu_d = \dfrac{D_H}{\Lambda^2}$ is the effective frequency of diffusive losses (where D_H is the diffusion coefficient and Λ is the diffusion length). The rate constants used in Eq. (4), the gas temperature, and the electron density N_e were determined from self-consistent simulations of a hydrogen discharge [13]. Though we are dealing with a discharge in a hydrogen–methane mixture, the use in Eq. (4) of the rate constants calculated for pure hydrogen is quite justified because the methane additive is small (up to a few percent) and, as follows from the experimental results presented in Fig. 3a, only slightly affect the concentration of atomic hydrogen.

The equations for all of the mixture components were supplemented with the term

$$\frac{\partial N_i}{\partial t} = \ldots - \frac{N_i}{\tau_p}, \tag{5}$$

where τ_p is the characteristic time during which the gas mixture was pumped out from the reactor. The time τ_p depends on the gas flow rate and is determined experimentally from the fading time of the argon emission lines after argon is stopped to be supplied into the reactor, while the flow rate of the hydrogen–methane mixture remains unchanged (as was noted in Section 3, argon was supplied into the reactor at a much lower rate than hydrogen). The model took into account the supply of molecular hydrogen and methane (CH$_4$) into the reactor. It was assumed that, at a constant pressure and temperature, the total density of gas particles was constant.

Looking aside from specific mechanisms for DF growth, the interaction of the gas components with the DF surface was described by model reactions that accounted for the deposition of carbon-containing species on the surface and the supply of carbon from this surface into the plasma volume.

In [25], the following formulas for the DF growth rate G and the relative density of diamond defects X_{def} were proposed:

$$G \propto \frac{[CH_3]_{sur}[H]_{sur}}{3 \times 10^{15} \text{ см}^{-3} + [H]_{sur}}, \quad X_{def} \propto \frac{G}{[H]_{sur}^2}, \tag{6}$$

where $[H]_{sur}$ and $[CH_3]_{sur}$ are the densities of hydrogen atoms and CH$_3$ molecules at the substrate surface. At moderate atomic-hydrogen densities typical of microwave reactors [25], we have $G \propto [CH_3]_{sur}[H]_{sur}$. It was assumed that, at a constant gas density, the particle density near the surface was proportional to that calculated in the plasma volume. Hence, the loss of carbon atoms in the model was described by the equation

$$\frac{d[CH_3]}{dt} = -k_a[CH_3][H] = -\frac{[CH_3]}{\tau_{CH_3}}, \tag{7}$$

where τ_{CH_3} is characteristic loss time of CH$_3$ radicals from the discharge volume due to DF deposition.

In a microwave reactor, the influx of carbon atoms from the surface into the discharge volume is mainly due to thermal desorption [25]. Since the equilibrium hydrocarbon composition is reached fairly fast, it is no matter in which form carbon arrives from the surface at the discharge region. Hence, the influx of carbon from the surface can be represented in the form

$$\frac{d[CH_3]}{dt} = I_C. \tag{8}$$

The parameters τ_{CH_3} and I_C, entering into Eqs. (7) and (8), were determined from the measured dependence of the emission intensity on the gas flow rate in the reactor (Fig. 4). Note that these parameters can vary significantly in different experiments because they are affected, e.g., by the surface temperature of the growing film and the presence of carbon on the reactor wall.

A comparison of the experimental data and simulation results presented in Fig. 4a shows that the measured dependences of the intensity ratios on the gas flow rate are adequately described by the model at $\tau_{CH_3} = 0.01$ s. Using the τ_{CH_3} value thus determined, one can estimate the DF growth rate as the number of carbon atoms deposited on the substrate per unit time,

$$G\left[\frac{mg}{h}\right] = \frac{[CH_3]V_{pl}M_C}{\tau_{CH_3}}, \tag{9}$$

where V_{pl} is the volume occupied by the microwave discharge plasma (it is determined experimentally from the visible size of the discharge), $[CH_3]$ is the calculated density of CH$_3$ radicals, and M_C is the mass of a carbon atom. For the flow rate of the 1 %CH$_4$/H$_2$ mixture equal to 200 sccm, the DF growth rate estimated by formula (9) (with allowance for the DF surface area and the diamond specific density) is 0.3 μm/h, which is close to the measured value of 0.4 μm/h (Fig. 5).

A comparison of the experimental data and simulation results presented in Fig. 4b shows that, for a zero content of methane, the measured dependences of the intensity ratios on the gas flow rate are adequately described by the model at a carbon flow rate from the surface of $I_C = 1.7 \times 10^{12}$ sccm.

Figure 7 shows the composition of the microwave discharge plasma as a function of the methane percentage in the gas mixture for a gas temperature of 2500 K and pressure of 90 Torr. It can be seen that, in accordance with the experimental data [26] and simulation results [19], the methane entering the reactor almost completely converts into acetylene (C_2H_2). In [26], the conversion of methane into acetylene was attributed to the high gas temperature and the superequilibrium atomic hydrogen concentration arising due to the dissociation of molecular hydrogen in plasma. The concentrations of all the C_2-containing hydrocarbons are proportional to the acetylene concentration, whereas the concentrations of hydrocarbons containing one C atom are proportional to the concentration of methyl radical CH_3. This relation between the concentrations of the carbon-containing components also takes place when other parameters (such as the pressure and gas-mixture flow rate) are varied. A linear relation between the emission intensity of C_2 and the concentration of C_2H_2 was observed experimentally in [17].

At a the zero methane percentage in the gas mixture, the concentrations of carbon-containing radicals are nonzero (see Fig. 7) due to the influx of carbon atoms from the substrate surface and the discharge chamber wall (see formula (8)).

Figures 3 and 4 also show the experimental data and simulation results on the concentration ratios corresponding to the ratios of the emission intensities. It can be seen that the model adequately describes the experimentally observed dependences.

5. DISCUSSION OF EXPERIMENTAL AND SIMULATION RESULTS

It follows from the above results (see Figs. 3–5) that the processes in a CVD reactor can be monitored by measuring the intensity ratios between different emission lines of the hydrocarbon plasma components. Which pair of lines should be used depends on a particular problem. Generally, the intensity ratio is proportional to the concentration ratio of the corresponding mixture components. For example, the concentration ratio $[C_2]/[H]$ increases linearly with methane percentage and almost linearly with pressure. Methane entering the reactor converts via a chain of reactions into acetylene (C_2H_2), which is the main carbon-containing component at sufficiently high gas temperatures. C_2 radicals are produced from acetylene via the reactions $C_2H_2 \longleftrightarrow C_2H \longleftrightarrow C_2$ (Fig. 6). Therefore, the concentration ratio $[C_2]/[H]$ is proportional to the degree of dissociation of hydrogen, $[H]/[H_2]$, and to the ratio $[C_2H_2]/[H_2]$ (i.e., to the established percentage of carbon in the mixture). Thus, we have [$\dfrac{[C_2]}{[H]}$ =
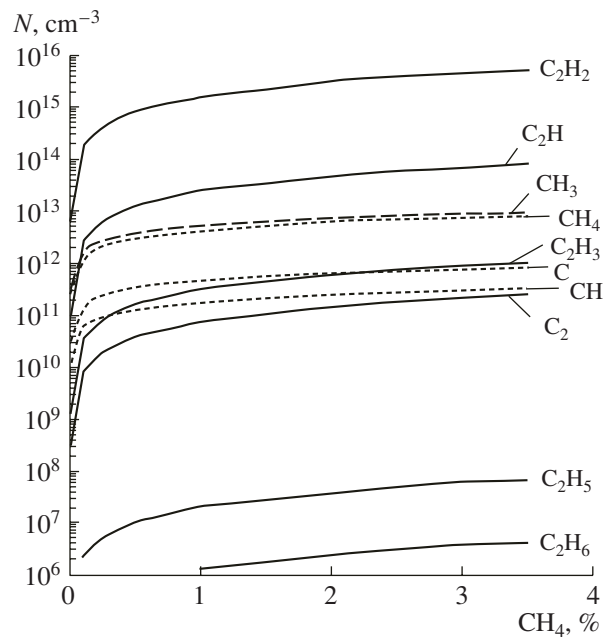

N, cm^{-3}

Fig. 7. Calculated densities of different components as functions of the methane percentage in the gas mixture.

$\dfrac{[H]}{[H_2]}\dfrac{[C_2H_2]}{[H_2]}$]. Hence, when the degree of dissociation of H_2 is constant, the $[C_2]/[H]$ ratio is a linear function of the methane percentage in the mixture. The carbon content in a $[C_2H_2]/[H_2]$ mixture changes only slightly with pressure, and the $[C_2]/[H]$ ratio increases nearly in proportion to the degree of dissociation of hydrogen (Fig. 3b).

The intensity ratio I_{C_2}/I_{H_α} was used in [8] to monitor the DF growth rate. It follows from the above considerations that this ratio takes into account both factors affecting the film growth rate: the carbon content and the degree of dissociation of hydrogen.

Methyl radical CH_3 participates in the chain of fast reactions $CH_4 \longleftrightarrow CH_3 \longleftrightarrow CH_2 \longleftrightarrow CH \longleftrightarrow C$; hence, the concentrations of hydrocarbons containing one C atom rapidly reach their equilibrium values. Therefore, there is a certain algebraic relationship between these concentrations and the $[H]/[H_2]$ ratio, from which it follows that $[CH_3][H] \propto \dfrac{[CH]}{[H]}[H_2]^2$. Taking into account formula (6), we can conclude that, at a constant gas density, there is a correlation between the $[CH]/[H]$ ratio (and the corresponding ratio of the emission intensities) and the DF growth rate (see Fig. 5). At a given gas flow rate, the hydrocarbon content in the mixture is determined by the balance between the supply of methane into the reactor, on one hand, and the pumping-out of the reaction products and their deposition on the DF surface, on the other hand. In the range

of gas flow rates under study, the dependence of the ratio $I_{CH}/I_{H\gamma}$ on the gas flow rate (Fig. 4) resembles the dependence of the DF growth rate on the gas flow rate observed in [27].

The calculated ratio $[CH_3][H]$ increases rapidly with pressure. In [28], it was experimentally shown that the DF growth rate also rapidly increases with pressure. The intensity ratio $I_{CH}/I_{H\gamma}$ and the concentration ratio $[CH]/[H]$ vary slowly with increasing pressure (see Fig. 3b). However, if we assume that the gas temperature in the discharge depends slightly on the pressure, whereas the degree of dissociation of hydrogen is low, then the concentration product $[CH_3][H]$ will be related to the $[CH]/[H]$ ratio as $[CH_3][H] \propto \dfrac{[CH]}{[H]} [H_2]^2 \sim \dfrac{[CH]}{[H]} p^2$. Thus, taking into account the pressure effect, the intensity ratio $I_{CH}/I_{H\gamma}$ can again be used to control the DF growth rate. Note that variations in the gas pressure affect such important parameters as the surface temperature; the plasma volume; and, consequently, the interaction area, which determine the plasma–surface interaction and, accordingly, the mixture chemical composition and the DF growth. It is practically impossible to take into account these variations in the above numerical model.

In [6], the DF quality was monitored by using the I_{C_2}/I_{CH} ratio. In simulations, the corresponding concentration ratio is proportional to the concentration ratio of C_2H_2 and CH_3: [$\dfrac{[C_2]}{[CH]} \propto \dfrac{[C_2H_2]}{[CH_3]}$]. Taking into account that carbon is almost completely incorporated in acetylene, the I_{C_2}/I_{CH} ratio also determines the fraction of carbon incorporated in methyl radical CH_3. Therefore, this ratio characterizes the relative contributions of different mechanisms to the growth of a DF from methyl radicals and acetylene [29, 30]. In [6], the effect of the methane percentage in the mixture on both the DF quality and the intensity ratio I_{C_2}/I_{CH} was investigated. It was found that an increase in the methane percentage leads to an increase in the fraction of the nondiamond phase and the I_{C_2}/I_{CH} ratio. This is why the ratio between the intensities of these lines is proposed to be used to monitor the quality of the produced DFs. As the methane percentage increases, the concentrations of C_2-containing hydrocarbons increase more rapidly than the concentrations of hydrocarbons containing one C atom (see Figs. 3a and 7). This increase is accompanied (to a certain extent) by an increase in the DF growth rate. According to [25], the concentration of DF defects at a constant density of atomic hydrogen is proportional to the DF growth rate. Hence, an increase in the methane flow rate leads to an increase in the DF growth rate and the corresponding decrease in the DF quality, as

well as to an increase in the I_{C_2}/I_{CH} ratio. When another discharge parameters affecting the concentration of atomic hydrogen are varied, the relation between the I_{C_2}/I_{CH} ratio and the DF quality can be more complicated.

6. CONCLUSIONS

The above experimental and simulation results led to the following conclusions. The DF growth can be monitored by using the intensity ratios of different pairs of emission lines. The line intensities (as well as their ratios) depend on many parameters. The concentrations of different carbon-containing components are determined by the degree of dissociation of hydrogen and the competition between the following processes: the supply of carbon into the reactor, the influx of carbon from the substrate surface and discharge chamber wall, the pumping-out of the gas mixture, and the deposition of carbon on the substrate and reactor wall in the form of a DF. The choice of a specific pair of emission lines for monitoring the process of DF deposition depends on experimental conditions. The DF growth rate correlates with the intensity ratio I_{CH}/I_H. The ratio I_{C_2}/I_H characterizes the equilibrium content of carbon and the degree of dissociation of hydrogen. The ratio I_{C_2}/I_{CH} is proportional to the concentration ratio of C_2H_2 and CH_3 and, under certain conditions, characterizes the DF quality and the relative contributions of different mechanisms to the DF growth.

REFERENCES

1. C. J. Erickson, W. B. Jameson, J. Watts-Cain, et al., Plasma Sources Sci. Technol. **5**, 761 (1996).

2. S. M. Leeds, P. W. May, E. Bartlett, et al., Diamond Relat. Mater. **8**, 1377 (1999).

3. M. J. Wouters, J. Khachan, I. S. Falconer, and B. W. James, J. Phys. D **31**, 2004 (1998).

4. Y. Liao, C. H. Li, Z. Y. Ye, et al., Diamond Relat. Mater. **9**, 1716 (2000).

5. J. Cui and R. J. Fang, J. Appl. Phys. **81**, 2856 (1997).

6. V. V. Dvorkin, N. N. Dzbanovskiĭ, P. V. Minakov, et al., Fiz. Plazmy **29**, 851 (2003) [Plasma Phys. Rep. **29**, 789 (2003)].

7. T. Vandevelde, T. D. Wu, C. Quaeyhaegens, et al., Thin Solid Films **340**, 159 (1999).

8. E. Sevillano, in *Low-Pressure Synthetic Diamond*, Ed. by B. Dischler and C. Wild (Springer-Verlag, Berlin, 1998), p. 11.

9. A. L. Vikharev, A. M. Gorbachev, V. A. Koldanov, and D. B. Radishchev, Fiz. Plazmy **31**, 376 (2005) [Plasma Phys. Rep. **31**, 338 (2005)].

10. X. Duten, A. Rousseau, A. Gicquel, and P. Leprince, J. Appl. Phys. **86**, 5299 (1999).

11. V. A. Koldanov, A. L. Vikharev, A. M. Gorbachev, et al., in *Proceedings of the 6th International Workshop on Strong Microwaves in Plasmas, Nizhny Novgorod, 2006*, p. 767.

12. V. N. Ochkin, *Spectroscopy of Low-Temperature Plasmas* (Fizmatlit, Moscow, 2006) [in Russian].

13. V. A. Koldanov, A. M. Gorbachev, A. L. Vikharev, and D. B. Radishchev, Fiz. Plazmy **31**, 1038 (2005) [Plasma Phys. Rep. **31**, 965 (2005)].

14. T. A. Grotjohn, J. Asmussen, J. Sivagnaname, et al., Diamond Relat. Mater. **9**, 322 (2000).

15. A. N. Goyette, J. E. Lawler, L. W. Anderson, et al., Plasma Sources Sci. Technol. **7**, 149 (1998).

16. M. Hiramatsu, K. Kato, C. H. Lau, et al., Diamond Relat. Mater. **12**, 365 (2003).

17. C. Benndorf, P. Joeris, and R. Kroger, Pure Appl. Chem. **66**, 1195 (1994).

18. P. John, J. R. Rabeau, and J. I. B. Wilson, Diamond Relat. Mater. **11**, 608 (2002).

19. D. G. Goodwin and J. E. Butler, in *Handbook of Industrial Diamonds and Diamond Films*, Ed. by M. A. Prelas, G. Popovici, and L. K. Bigelow (Marcel Dekker, New York, 1998), p. 527.

20. R. A. Akhmedzhanov, A. L. Vikharev, A. M. Gorbachev, et al., Diamond Relat. Mater. **11**, 579 (2002).

21. D. L. Baulch, C. J. Cobos, R. A. Cox, et al., Combust. Flame **98**, 59 (1994).

22. Yu. A. Mankelevich, A. T. Rakhimov, and N. V. Suetin, Fiz. Plazmy **21**, 921 (1995) [Plasma Phys. Rep. **21**, 872 (1995)].

23. http://www.me.berkeley.edu/gri_mech/

24. http://kinetics.nist.gov/

25. D. G. Goodwin, J. Appl. Phys. **74**, 6888, 6895 (1993).

26. T. A. Grotjohn and J. Asmussen, in *Diamond Films Handbook*, Ed. by J. Asmussen, and D. K. Reinhard (Marcel Dekker, New York, 2002), p. 211.

27. V. Ralchenko, I. Sychov, I. Vlasov, et al., Diamond Relat. Mater. **8**, 189 (1999).

28. V. Mortet, A. Kromka, R. Kravets, et al., Diamond Relat. Mater. **13**, 604 (2004).

29. M. P. D'Evelyn, J. D. Graham, and L. R. Martin, J. Crystal Growth **231**, 506 (2001).

30. M. P. D'Evelyn, J. D. Graham, and L. R. Martin, Diamond Relat. Mater. **10**, 1627 (2001).

Translated by N.N. Ustinovskiĭ